OPTIMAL OFDMA SUBCARRIER, RATE, AND POWER ALLOCATION FOR ERGODIC RATES MAXIMIZATION WITH IMPERFECT CHANNEL KNOWLEDGE

Ian C. Wong and Brian L. Evans

The University of Texas at Austin, Austin, Texas 78712
Email: {iwong,bevans}@ece.utexas.edu

ABSTRACT

Previous research efforts on OFDMA resource allocation have typically assumed the availability of perfect channel state information (CSI). Unfortunately, this is unrealistic, primarily due to channel estimation errors, and more importantly, channel feedback delay. In this paper, we develop optimal resource allocation algorithms for OFDMA systems assuming the availability of only partial (imperfect) CSI. We consider ergodic weighted sum discrete rate maximization subject to total power constraints. We approach this problem using a dual optimization framework, allowing us to solve this problem with $\mathcal{O}(MK)$ complexity per symbol for an OFDMA system with K used subcarriers and M active users, while achieving relative optimality gaps of less than 10^{-3} (99.999% optimal).

Index Terms: Multiaccess communication, Information rates, Resource management, Optimization methods, Uncertain systems

1. INTRODUCTION

Next-generation broadband wireless system standards, e.g. 3GPP-Long Term Evolution (LTE) [1], consider Orthogonal Frequency Division Multiple Access (OFDMA) as the preferred physical layer multiple access scheme, esp. for the downlink. The problem of assigning the subcarriers, rates, and powers to the different users in an OFDMA system has been an area of active research, (see e.g. [2]). A common underlying assumption among these works is that the channel state information (CSI) of the users are known perfectly. This assumption is quite unrealistic due to channel estimation errors, and more importantly, channel feedback delay. Thus, in this paper, we focus on the case where only imperfect (partial) CSI is available.

The effect of imperfect CSI for rate maximization in wireless systems has been quite well studied for single-user OFDM systems [3]. However, no work to the best of the authors's knowledge considered the multiuser OFDM case. In the multiuser OFDM (or OFDMA) case, the difficulty arises from the fact that the exclusive subcarrier assignment restriction (i.e. only one user is allowed to transmit on each subcarrier) renders the problem to be combinatorial in nature. Fortunately, in our recent work on optimal resource allocation for ergodic rate maximization in OFDMA systems with perfect CSI [4], we have shown that using a dual optimization approach, the problem can be solved with just $\mathcal{O}(MK)$ complexity per symbol for an OFDMA system with M active users and K used subcarriers. Furthermore, our solution results in relative optimality gaps of less than 10^{-4} in typical scenarios, thereby supporting us to claim *practical optimality*. Using a similar dual optimization approach, we relax the assumption of perfect CSI and formulate and solve the problem assuming the availability of imperfect CSI. We show that by using the dual optimization framework, we can solve the imperfect CSI problem with relative optimality gaps of less than 10^{-3} in cases of

practical interest. Note that the dual optimization framework has also been used in the DSL context in [5].

2. SYSTEM MODEL

We consider a single OFDMA base station with K-subcarriers and M-users indexed by the set $\mathcal{K} = \{1, \ldots, k, \ldots, K\}$ and $\mathcal{M} = \{1, \ldots, m, \ldots, M\}$ (typically $K \gg M$) respectively. We assume an average transmit power of $\bar{P} > 0$, bandwidth B, and noise density N_0. The received signal vector for the mth user at the nth OFDM symbol is given as

$$\boldsymbol{y}_m[n] = \mathbf{G}_m[n]\mathbf{H}_m[n]\boldsymbol{x}_m[n] + \boldsymbol{w}_m[n] \qquad (1)$$

where $\boldsymbol{y}_m[n]$ and $\boldsymbol{x}_m[n]$ are the K-length received and transmitted complex-valued signal vectors; $\mathbf{G}_m[n]$ is the diagonal gain allocation matrix with diagonal elements $[\mathbf{G}_m[n]]_{kk} = \sqrt{p_{m,k}[n]}$; $\boldsymbol{w}_m[n] \sim \mathcal{CN}(\mathbf{0}, \sigma_w^2 \boldsymbol{I}_K)$ with noise variance $\sigma_w^2 = N_0 B/K$ is the white zero-mean, circular-symmetric, complex Gaussian (ZMCSCG) noise vector; and $\mathbf{H}_m[n] = \mathrm{diag}\{\boldsymbol{h}_m[n]\}$ is the diagonal channel response matrix, where $\boldsymbol{h}_m = [h_{m,1}[n], \ldots, h_{m,K}[n]]^T$ and where

$$h_{m,k}[n] = \sum_{i=1}^{N_t} g_{m,i}[n] e^{-j2\pi \tau_i k \Delta f}. \qquad (2)$$

are the complex-valued frequency-domain wireless channel fading random processes, given as the discrete-time Fourier transform of the N_t time-domain multipath taps $g_{m,i}[n]$ with time-delay τ_i and subcarrier spacing Δf. The $g_{m,i}[n]$ are the time-domain fading channel taps modeled as stationary and ergodic discrete-time random processes, with identical normalized temporal autocorrelation function

$$r_m[\Delta] = \frac{1}{\sigma_{m,i}^2} \mathbb{E}\{g_{m,i}[n]g_{m,i}^*[n+\Delta]\}, \quad i = 1, \ldots, N_t \qquad (3)$$

with tap powers $\sigma_{m,i}^2$, which we assume to be independent across the fading paths i and across users m. Since $g_{m,i}[n]$ is stationary, $h_{m,k}[n]$ is also stationary, and the distribution of $\boldsymbol{h}_m[n]$ is independent of symbol index n.

Assuming that the time domain channel taps are independent ZMCSCG random variables $g_{m,i} \sim \mathcal{CN}(0, \sigma_{m,i}^2)$, then from (2),

$$\boldsymbol{h}_m \sim \mathcal{CN}(\mathbf{0}_K, \boldsymbol{\Sigma}_{\boldsymbol{h}_m})$$
$$\boldsymbol{\Sigma}_{\boldsymbol{h}_m} = \mathbf{W}\boldsymbol{\Sigma}_{\boldsymbol{g}_m}\mathbf{W}^H \qquad (4)$$

where $\mathbf{W}$ is the $K \times N_t$ DFT matrix with $[\mathbf{W}]_{k,i} = e^{-j2\pi \tau_i k \Delta f}$ and $\boldsymbol{\Sigma}_{\boldsymbol{g}_m} = \mathrm{diag}\{\sigma_{m,1}^2, \ldots, \sigma_{m,N_t}^2\}$ is an $N_t \times N_t$ diagonal matrix of the time-domain path covariances. We model partial CSI as

$$\boldsymbol{h}_m = \hat{\boldsymbol{h}}_m + \hat{\boldsymbol{e}}_m \qquad (5)$$

where $\hat{\boldsymbol{h}}_m \sim \mathcal{CN}\left(\mathbf{0}_K, \boldsymbol{\Sigma}_{\boldsymbol{h}_m} - \hat{\boldsymbol{\Sigma}}_m\right)$ is the estimated channel vector and $\hat{\boldsymbol{e}} \sim \mathcal{CN}(\mathbf{0}_K, \hat{\boldsymbol{\Sigma}}_m)$ is the estimation error vector with

$$\hat{\boldsymbol{\Sigma}}_m = \boldsymbol{\Sigma}_{\boldsymbol{h}_m} - (\mathbf{r}_m^T \otimes \boldsymbol{\Sigma}_{\boldsymbol{h}_m})(\mathbf{R}_m \otimes \boldsymbol{\Sigma}_{\boldsymbol{h}_m} + \sigma_e^2 \mathbf{I}_{PK})^{-1}(\mathbf{r}_m^T \otimes \boldsymbol{\Sigma}_{\boldsymbol{h}_m})^H$$

as the error covariance matrix for a Pth order MMSE predictor for the channel with pilot spacing D_t, where $[\mathbf{R}_m]_{i,j} = r_m[(i-j)D_t]$, $\mathbf{r}_m^T = [r_m[D_t], \ldots, r_m[PD_t]]$, and $\otimes$ is the Kronecker product.

We assume that the marginal fading distribution on subcarrier k conditioned on the estimated channel is a non-zero mean complex Gaussian random variable given as $h_{m,k}|\hat{h}_{m,k} \sim \mathcal{CN}(\hat{h}_{m,k}, \hat{\sigma}_{m,k}^2)$ where $\hat{h}_{m,k}$ is the estimated complex channel gain and $\hat{\sigma}_{m,k}^2$ is the estimation error variance for that subcarrier. Thus, the channel-to-noise ratio (CNR) $\gamma_{m,k} = |h_{m,k}|^2/\sigma_w^2$ conditioned on $\hat{\gamma}_{m,k} = |\hat{h}_{m,k}|^2/\sigma_w^2$ is in turn a non-central Chi-squared distributed random variable with two degrees of freedom with pdf [6, Eq. 2-1-118]

$$f_{\gamma_{m,k}}(\gamma_{m,k}|\hat{\gamma}_{m,k}) = \frac{1}{\rho_{m,k}} e^{-\frac{\hat{\gamma}_{m,k}+\gamma_{m,k}}{\rho_{m,k}}} I_0\left(\frac{2}{\rho_{m,k}}\sqrt{\hat{\gamma}_{m,k}\gamma_{m,k}}\right)$$
$$(6)$$

where I_0 is the zeroth-order modified Bessel function of the first kind, and $\rho_{m,k} = \hat{\sigma}_{m,k}^2/\sigma_w^2$ is the ratio of the estimation error variance to the ambient noise variance.

3. DISCRETE RATE MAXIMIZATION WITH PARTIAL CSI

3.1. Problem Formulation

In the discrete rate case, the data rate of the kth subcarrier for the mth user can be given by the following staircase function

$$R_{m,k}^d(p_{m,k}\gamma_{m,k}) = \begin{cases} 0, & p_{m,k}\gamma_{m,k} < \eta_0 \\ r_1, & \eta_0 \leq p_{m,k}\gamma_{m,k} < \eta_1 \\ \vdots & \vdots \\ r_L, & \eta_{L-1} \leq p_{m,k}\gamma_{m,k} < \eta_L \equiv \infty \end{cases}$$
$$(7)$$

where $\{r_l\}_{l \in \mathcal{L}}$, $\mathcal{L} = \{1, \ldots, L\}$ are the L available discrete information rates in increasing order, and $\{\eta_l\}_{l=0}^{L-1}$ are the SNR boundaries chosen in such a way that the information rate r_l is supportable subject to an instantaneous BER constraint. In the perfect CSI case, the candidate power allocation function that satisfies the BER constraint for each possible rate r_l is simply multi-level fading inversion (MFI), i.e. $p_{m,k}^{(l)} = \eta_l/\gamma_{m,k}$ [4]. This allows us to do away with having a BER function, since all that we require are the SNR rate region boundaries η_l which can be computed offline. However, with imperfect CSI, the average rate is given as

$$\bar{R}_{m,k} = \sum_{l \in \mathcal{L}} r_l P\left(\eta_{l-1} \leq p_{m,k}\gamma_{m,k} < \eta_l | \hat{\gamma}_{m,k}\right)$$
$$(8)$$

Since we do not have the perfect CSI information $\gamma_{m,k}$, simply performing MFI on the imperfect CSI $\hat{\gamma}_{m,k}$ does not guarantee satisfaction of the BER constraint, and is illustrated in Section 4.

With the imperfect CSI assumption, we require a BER function that can be expressed in terms of the SNR $p_{m,k}\gamma_{m,k}$ for a given r_l in order to enforce the *average* BER constraint. Suppose that we have this BER function for a given rate r_l denoted as $\text{BER}_l(p_{m,k}\gamma_{m,k})$, which could be derived using theoretical analysis or curve fitting from empirical data, the average BER constraint can be written as

$$\mathbb{E}\left\{\text{BER}_l(p_{m,k}\gamma_{m,k})|\hat{\gamma}_{m,k}\right\} = \overline{\text{BER}}$$
$$(9)$$

Solving for $p_{m,k}$ in (9) for each $l \in \mathcal{L}$, we have L power allocation functions to choose from.

In order to simplify our development, we derive a closed-form expression for (9) assuming the fading distributions derived in Section 2, and a representative BER prototype function that has been empirically shown to fit a lot of practical scenarios (see e.g. [7]). This prototype BER function is given by

$$\text{BER}_l(p_{m,k}\gamma_{m,k}) = a_l \exp\left(-b_l p_{m,k}\gamma_{m,k}\right)$$
$$(10)$$

where a_l and b_l are constants that are searched to fit the actual BER function for each r_l. For example, if we assume a Grey-coded square 2^{r_l}-QAM modulation scheme in AWGN, the BER function can be approximated to within 1-dB for $r_l \geq 2$ and BER $\leq 10^{-3}$ with $a_l = 0.2$ and $b_l = 1.6/(2^{r_l}-1)$ [7]. Using (10) in (9) with the pdf in (6), we have after some algebraic manipulation

$$\mathbb{E}\{\text{BER}_l(p_{m,k}\gamma_{m,k})|\hat{\gamma}_{m,k}\} = \qquad (11)$$
$$\hat{a}_{m,k}^{(l)} \int_0^\infty \exp\left(-x\left(\hat{b}_{m,k}^{(l)}p_{m,k}+1\right)\right) I_0\left(2\sqrt{K_{m,k}x}\right) dx$$

where $x = \gamma_{m,k}/\rho_{m,k}$, $K_{m,k} = \hat{\gamma}_{m,k}/\rho_{m,k}$, and

$$\hat{a}_{m,k}^{(l)} = a_l \exp\left(-K_{m,k}\right)$$
$$\hat{b}_{m,k}^{(l)} = b_l \rho_{m,k}$$
$$(12)$$

Eq. (11) can be interpreted as the Laplace transform of $I_0(2\sqrt{K_{m,k}x})$ with parameter $s = \hat{b}_{m,k}^{(l)}p_{m,k}+1$, which is given in [8, Eq. 29.3.81]. Hence, a closed form expression for (11) can be written as

$$\mathbb{E}\{\text{BER}_l(p_{m,k}\gamma_{m,k})|\hat{\gamma}_{m,k}\}$$
$$= \frac{\hat{a}_{m,k}^{(l)}}{\hat{b}_{m,k}^{(l)}p_{m,k}+1} \exp\left(\frac{K_{m,k}}{\hat{b}_{m,k}^{(l)}p_{m,k}+1}\right)$$
$$(13)$$

Equating (13) with the target $\overline{\text{BER}}$, we arrive at the closed form expression for the candidate power allocation function given the estimated CNR $\hat{\gamma}_{m,k}$ and data rate r_l

$$\hat{p}_{m,k}^{(l)} = \frac{1}{\hat{b}_{m,k}^{(l)}}\left(\frac{K_{m,k}}{W\left(\overline{\text{BER}}K_{m,k}/\hat{a}_{m,k}^{(l)}\right)} - 1\right)$$
$$(14)$$

where $W(x)$ is the *Lambert-W* function, which is the solution to the transcendental equation $W(x)e^{W(x)} = x$. This function is ubiquitous in the physical sciences, and efficient algorithms have been extensively studied for its computation [9]. It is important to emphasize that (14) gives us the power allocation value that fulfills the average BER constraint when r_l is chosen as the rate for a particular user m and subcarrier k given imperfect CSI $\hat{\gamma}_{m,k}$. Fig. 1 shows the power allocation as a function of the estimated CNR $\hat{\gamma}_{m,k}$ for uncoded $4-$QAM and $64-$QAM for various $\rho_{m,k}$. We also plot the power allocation function when treating the $\hat{\gamma}_{m,k}$ as perfect, i.e. $p_{m,k}^{(l)} = \eta_l/\hat{\gamma}_{m,k}$ called multi-level fading inversion on imperfect CSI (Imperfect CSI-MFI). We can see that as $\rho_{m,k}$ decreases (prediction accuracy increases), the power allocation function approaches that of Imperfect CSI-MFI. On the other hand, a higher $\rho_{m,k}$ requires higher power in order to ensure the average BER requirement is met, especially for low estimated CNR $\hat{\gamma}_{m,k}$. Note also that the power allocation functions approach the Imperfect CSI-MFI value as $\hat{\gamma}_{m,k}$ becomes large, despite the value of $\rho_{m,k}$.

Using (14) in (8), the average rate given that r_l is chosen as the transmission rate can be written as

$$\bar{R}_{m,k}(r_l) = \sum_{i \in \mathcal{L}} r_i P\left(\eta_{i-1} \le \hat{p}_{m,k}^{(l)}\gamma_{m,k} < \eta_i | \hat{\gamma}_{m,k}\right) \quad (15)$$

$$= \sum_{i \in \mathcal{L}} r_i P\left(\frac{\eta_{i-1}}{\hat{p}_{m,k}^{(l)}} \le \gamma_{m,k} < \frac{\eta_i}{\hat{p}_{m,k}^{(l)}} \Big| \hat{\gamma}_{m,k}\right)$$

$$= \sum_{i \in \mathcal{L}} r_i \left(F_{\gamma_{m,k}}\left(\frac{\eta_i}{\hat{p}_{m,k}^{(l)}} \Big| \hat{\gamma}_{m,k}\right) - F_{\gamma_{m,k}}\left(\frac{\eta_{i-1}}{\hat{p}_{m,k}^{(l)}} \Big| \hat{\gamma}_{m,k}\right) \right)$$

From [6, Eq. 2.1-124], we have the following closed-form expression for the cdf of a non-central Chi-squared random variable

$$F_{\gamma_{m,k}}\left(x | \hat{\gamma}_{m,k}\right) = 1 - Q\left(\sqrt{\frac{2\hat{\gamma}_{m,k}}{\rho_{m,k}}}, \sqrt{\frac{2x}{\rho_{m,k}}}\right) \quad (16)$$

where $Q(a,b)$ is the Marcum-Q function. Using (16) in (15), we have a closed-form expression for the average rate for user m and subcarrier k given a choice of transmission rate r_l.

Considering the above development, we can think of our decision variables in this case as a vector of rate allocation indices $\boldsymbol{l} = [\boldsymbol{l}_1^T, \dots, \boldsymbol{l}_K^T]^T$, $\boldsymbol{l}_k^T = [l_{1,k}, \dots, l_{M,k}]^T$ and $l_{m,k} \in \{0, 1, \dots, L\}$. The exclusive subcarrier assignment restriction can be written as $\boldsymbol{l}_k \in \mathcal{L}_k$, where

$$\mathcal{L}_k = \{l_{m,k} \in \{0, 1, \dots, L\} | l_{m,k} l_{m',k} = 0; \forall m \ne m'\} \quad (17)$$

For notational convenience, we let $\boldsymbol{l} \in \mathcal{L} = \mathcal{L}_1 \times \cdots \times \mathcal{L}_K$ denote the space of allowable rate allocation indices for all subcarriers. Note that a decision of $l_{m,k} = 0$ means that neither rate nor power is transmitted on subcarrier k by user m. Thus, we can define $\bar{R}_{m,k}(r_0) \equiv 0$ and $\hat{p}_{m,k}^{(0)} \equiv 0$. The discrete weighted sum rate maximization problem with partial CSI is then formulated as

$$f_d^* = \max_{\boldsymbol{l} \in \mathcal{L}} \sum_{m \in \mathcal{M}} w_m \sum_{k \in \mathcal{K}} \bar{R}_{m,k}(r_{l_{m,k}})$$

$$\text{s.t.} \sum_{m \in \mathcal{M}} \sum_{k \in \mathcal{K}} \hat{p}_{m,k}^{(l_{m,k})} \le \bar{P} \quad (18)$$

3.2. Dual Optimization Framework

The dual problem of (18) can be written as (see e.g. [4])

$$g_d^* = \min_{\lambda \ge 0} \lambda \bar{P} + \sum_{k \in \mathcal{K}} \max_{m \in \mathcal{M}} \max_{l \in \mathcal{L} \cup \{0\}} \bar{R}_{m,k}(r_l) - \lambda \hat{p}_{m,k}^{(l)} \quad (19)$$

where we can use a univariate line-search method such as Golden-section search to compute for the optimum multiplier λ_d^*. Note that neither (14) nor (15) depend on λ. Hence, we can pre-compute these quantities for all $l \in \mathcal{L}$, $m \in \mathcal{M}$, and $k \in \mathcal{K}$ before running the line search iterations. Using λ_d^*, we have

$$l_{m,k}^* = \arg\max_{l \in \mathcal{L}} w_m \bar{R}_{m,k}(r_l) - \lambda_d^* \hat{p}_{m,k}^{(l)} \quad (20)$$

$$m_k^* = \arg\max_{m \in \mathcal{M}} w_m \bar{R}_{m,k}(r_{l_{m,k}^*}) - \lambda_d^* \hat{p}_{m,k}^{(l_{m,k}^*)} \quad (21)$$

$$p_{m,k}^* = \begin{cases} \hat{p}_{m,k}^{(l_{m,k}^*)}, & m = m_k^* \\ 0, & m \ne m_k^* \end{cases} \quad (22)$$

$$r_{m,k}^* = \begin{cases} r_{l_{m,k}^*}, & m = m_k^* \\ 0, & m \ne m_k^* \end{cases} \quad (23)$$

3.3. Complexity Analysis

Before running the line search iterations to compute for λ^* in (19), we need to compute MKL power allocation values (14) and average rate values (15) and store it in memory. This is followed by the search iterations which we assume to require I_λ, wherein each iteration requires $\mathcal{O}(MK)$ operations (19). The overall complexity order for the discrete rate resource allocation algorithm is thus $\mathcal{O}(MK(L + I_\lambda))$. Since L and I_λ are just constants independent of M and K, the complexity is $\mathcal{O}(MK)$.

4. RESULTS AND DISCUSSION

We present several numerical examples to substantiate our theoretical claims. Our simulations are roughly based on a 3GPP-LTE downlink [1] system with parameters given in Table 1. We simulate the frequency-selective Rayleigh fading channel using the ITU-Vehicular A channel model [10]. We assume Clarke's U-shaped power spectrum [11] for each multipath tap, resulting in the temporal autocorrelation function $r_m[\Delta] = J_0(2\pi \Delta F_d D_t(K_{fft} + L_{cp})/F_s)$ where $J_0(x)$ is the zeroth-order Bessel function of the first kind [8, Ch. 9]. To simulate imperfect CSI, we generate IID realizations of $\hat{\boldsymbol{h}}_m$ and its prediction error vector $\hat{\boldsymbol{e}}_m$ as discussed in Section 2. This allows us to also generate the "actual" channel $\boldsymbol{h}_m$ for the perfect CSI cases using (5).

Fig. 2 shows the discrete rate region for the optimal resource allocation algorithm assuming imperfect CSI (Imperfect CSI-Optimal). We also show the rate region achieved by using optimal resource allocation for discrete rates with perfect CSI (Perfect CSI-Optimal), which is essentially MFI [4], and by using MFI on the imperfect CSI (Imperfect CSI-MFI). Observe that due to the imperfect CSI assumption, Imperfect CSI-Optimal loses approximately 8% of the sum capacity when compared to Perfect CSI-Optimal. Observe also that Imperfect CSI-MFI results in a rate region that is quite close to the Perfect CSI-Optimal, and actually results in higher raw rates than the Imperfect CSI-Optimal. However, if we consider the average BER for each subcarrier shown in Fig. 3, Imperfect CSI-Optimal actually meets the average BER constraint of 10^{-3} (within $\pm 2\%$), but Imperfect CSI-MFI results in average BER violations of between $30 - 180\%$. This is because Imperfect CSI-MFI is equally aggressive in rate and power allocation even when the CSI prediction error is quite large. Our proposed Imperfect CSI-Optimal algorithm, on the other hand, is actually more conservative in rate and power allocation when the prediction MSE is large, thus allowing the average BER to be met. In a practical communications system, this would mean the difference of whether a packet is decoded successfully or not. Thus, using Imperfect CSI-MFI would result in unnecessary packet retransmissions and delays, and consequently decrease the throughput significantly. An explicit characterization in terms of throughput, however, is beyond the scope of this paper.

Table 2 shows the other relevant metrics of the optimal resource algorithms. The first column shows the average number of line-search iterations it took to converge to a tolerance of 10^{-4}, and the second column the relative optimality gaps[1] [12] [4]. We see that the relative optimality gaps are virtually zero, which allows us to claim optimality of the algorithms for all practical purposes.

Table 1. Simulation Parameters

Parameter	Value	Parameter	Value
Subcarriers (K_{fft})	64	Vehicular speed (V)	120 kph
Used Subcarriers (K)	33	Doppler frequency (F_d)	289 Hz
Bandwidth (B)	1.25 MHz	Prediction filter length (P)	4
Sampling Freq. (F_s)	1.92 MHz	Pilot spacing (D_t)	7
Carrier Freq. (F_c)	2.6 GHz	CP Length L_{cp}	6 samples

Table 2. Other Relevant Metrics

SNR	No. of Iterations (I_λ)	Relative Gap ($\times 10^{-4}$)
5	21.33	71.48
10	21.12	7.707
15	21.15	5.662

Fig. 3. Average BER for both users in each subcarrier for Imperfect CSI-Optimal and Imperfect CSI-MFI.
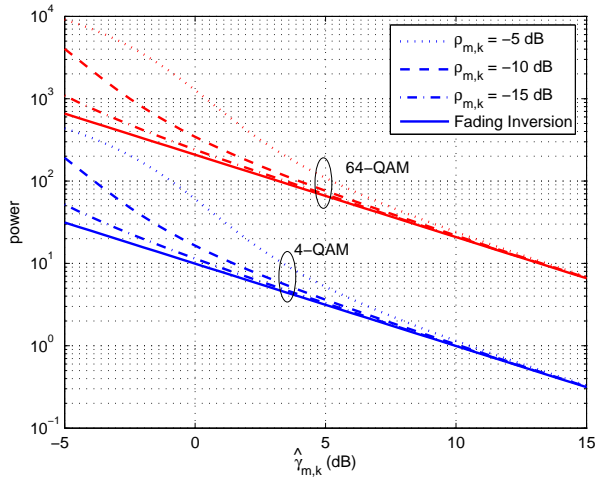

Fig. 1. Discrete rate power allocation as a function of estimated CNR ($\hat{\gamma}$) with $\gamma_0 = 1$ for various $\rho_{m,k}$.
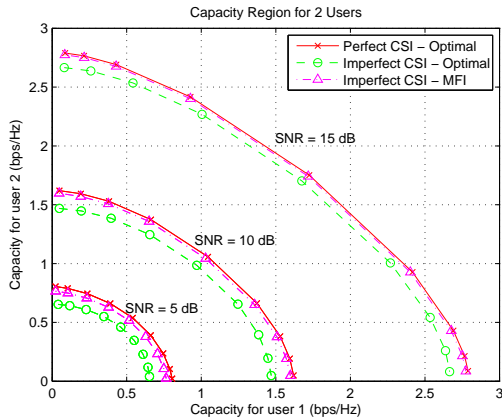

Fig. 2. 2-user capacity region for discrete rate optimal resource allocation with imperfect CSI. We also show the capacity region for optimal allocation with perfect CSI, and using multi-level fading inversion (MFI) on the imperfect CSI.
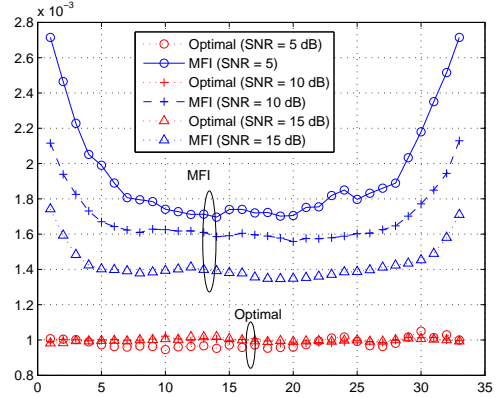
5. REFERENCES

[1] *3rd Generation Partnership Project, Technical Specification Group Radio Access Network; Physical layer aspects for evolved Universal Terrestrial Radio Access (UTRA)*, 3GPP Std. TR 25.814 v. 7.0.0, 2006.

[2] G. Song and Y. Li, "Cross-Layer Optimization for OFDM Wireless Networks Part II: Algorithm Development," *IEEE Trans. Wireless Commun.*, vol. 4, no. 2, pp. 625–634, Mar. 2005.

[3] Y. Yao and G. Giannakis, "Rate-Maximizing Power Allocation in OFDM Based on Partial Channel Knowledge," *IEEE Trans. Wireless Commun.*, vol. 4, no. 3, pp. 1073–1083, May 2005.

[4] I. C. Wong and B. L. Evans, "Optimal OFDMA resource allocation with linear complexity to maximize ergodic weighted sum capacity," in *Proc. IEEE Int. Conf. on Acoustics, Speech, and Signal Processing*, Honolulu, HI, April 2007.

[5] R. Cendrillon, W. Yu, M. Moonen, J. Verlinden, and T. Bostoen, "Optimal Multi-user Spectrum Balancing for Digital Subscriber Lines," *IEEE Trans. Commun.*, vol. 54, no. 5, May 2006.

[6] J. G. Proakis, *Digital communications*, 4th ed. McGraw-Hill, 2001.

[7] S. T. Chung and A. Goldsmith, "Degrees of freedom in adaptive modulation: a unified view," *IEEE Trans. Commun.*, vol. 49, no. 9, pp. 1561–1571, Sept. 2001.

[8] M. Abramowitz and I. A. Stegun, *Handbook of Mathematical Functions with Formulas, Graphs, and Mathematical Tables*, 10th ed. U.S. Govt. Print. Off., 1972.

[9] R. Corless, G. Gonnet, D. Hare, D. Jeffrey, and D. Knuth, "On the Lambert-W function," *Advances in Computational Mathematics*, vol. 5, no. 1, pp. 329–359, 1996.

[10] *Selection procedures for the choice of radio transmission technologies for the UMTS*, ETSI Std. TR 101 112 v. 3.2.0, 1998.

[11] G. L. Stüber, *Principles of Mobile Communication*, 2nd ed. Kluwer Academic, 2001.

[12] D. P. Bertsekas, *Nonlinear programming*, 2nd ed. Athena Scientific, 1999.